

Non-steady Accretion in Protostars

Zhaohuan Zhu¹, Lee Hartmann¹, and Charles Gammie^{2,3}

zhuzh@umich.edu, lhartm@umich.edu, gammie@illinois.edu

ABSTRACT

Observations indicate that mass accretion rates onto low-mass protostars are generally lower than the rates of infall to their disks; this suggests that much of the protostellar mass must be accreted during rare, short outbursts of rapid accretion. We explore when protostellar disk accretion is likely to be highly variable. While constant α disks can in principle adjust their accretion rates to match infall rates, protostellar disks are unlikely to have constant α . In particular we show that neither models with angular momentum transport due solely to the magnetorotational instability (MRI) nor gravitational instability (GI) are likely to transport disk mass at protostellar infall rates over the large range of radii needed to move infalling envelope material down to the central protostar. We show that the MRI and GI are likely to combine to produce outbursts of rapid accretion starting at a few AU. Our analysis is consistent with the time-dependent models of Armitage, Livio, & Pringle (2001) and agrees with our observational study of the outbursting object FU Ori.

Subject headings: accretion disks, stars: formation, stars: pre-main sequence

1. Introduction

The standard model of low-mass star formation posits the free-fall collapse of a protostellar molecular cloud core to a protostar plus disk during times of a few times 10^5 yr (e.g., Shu, Adams, & Lizano 1987), consistent with the statistics of protostellar objects in Taurus (Kenyon et al. 1990, 1994). To build up a star over these timescales requires a time-averaged infall rate of order $2 \times 10^{-6} - 10^{-5} M_{\odot} \text{ yr}^{-1}$, rates typically used in calculations of protostellar properties at the end of accretion (Stahler 1988; Hartmann, Cassen, & Kenyon 1997). The numerical simulations of dynamic star cluster formation by Bate et al. (2003) found that stars and brown dwarfs formed in burst lasting $\sim 2 \times 10^4$ years, implying infall rates of $\sim 10^{-4}$ to $10^{-5} M_{\odot} \text{ yr}^{-1}$. However, the accretion luminosity implied by such infall rates is considerably higher than typical observed protostellar

¹Dept. of Astronomy, University of Michigan, 500 Church St., Ann Arbor, MI 48105

²Dept. of Astronomy, University of Illinois Urbana-Champaign, 1002 W. Green St., Urbana, IL 61801

³Dept. of Physics, University of Illinois Urbana-Champaign

luminosities (Kenyon et al. 1990, 1994). This “luminosity problem” can be solved temporarily by piling up infalling matter in the circumstellar disk. Most of the mass must eventually be accreted onto the star, however. This requires major accretion events that are sufficiently short-lived that protostars are usually observed in quiescence.

This picture of highly time-dependent accretion is supported by observations. Individual knots in jets and Herbig-Haro objects, thought to be the result of outflows driven by accretion energy, argue for substantial disk variability (e.g., Bally, Reipurth, & Davis 2007). The FU Ori objects provide direct evidence for short episodes of rapid accretion in early stages of stellar evolution, with accretion rates of $10^{-4} M_{\odot} \text{ yr}^{-1}$ or more (Herbig 1977; Hartmann & Kenyon 1996), vastly larger than typical infall rates of $\lesssim 10^{-5} M_{\odot} \text{ yr}^{-1}$ for low-mass objects (e.g., Kenyon, Calvet, & Hartmann 1993; Furlan et al. 2008).

The mechanism driving FU Ori outbursts is not yet clear. A variety of models have been proposed: thermal instability (TI; Lin & Papaloizou 1985; Bell & Lin 1994); gravitational instability (GI; Vorobyov & Basu 2005, 2005); gravitational instability and activation of the magnetorotational instability (MRI; Armitage, Livio, & Pringle 2001; also Gammie 1999 and Book & Hartmann 2005); and even models in which planets act as a dam limiting downstream accretion onto the star (Clarke & Syer 1996; Lodato & Clarke 2004). Our recent analysis based on Spitzer IRS data (Zhu et al. 2007) led us to conclude that a pure TI model cannot work for FU Ori.

In view of the complexity of the problem and the physical uncertainties we adopt a schematic approach. We start with the (optimistic) assumption that protostellar accretion can be steady. We then show that the GI is likely to dominate in the outer disk, while the MRI is likely to be important in the inner disk, and that mismatches between the GI and MRI result in non-steady accretion for expected protostellar infall rates.¹ Our analysis agrees with the results found in the time-dependent outburst model of Armitage et al. (2001), and is consistent with our empirical analysis of the outbursting system FU Ori (Zhu et al. 2007). Although our results depend on simplified treatments of the GI and MRI, the overall picture is insensitive to parameter choices. We predict that above a critical infall rate protostellar disk accretion can be (relatively) steady; observational confirmation would help constrain mass transport rates by the GI and the MRI.

2. Overview

A disk with viscosity² ν will evolve at cylindrical radius r on a timescale

$$t_{\nu} \sim r^2 / \nu \tag{1}$$

¹GI and MRI here means turbulent states initiated by gravitational or magnetic instabilities, respectively.

²We use “viscosity” as shorthand for internal, localized transport of angular momentum by turbulence. We will also make the nontrivial assumption that external torques (e.g. MHD winds) can be neglected.

If this is comparable to the timescales over which mass is being added to the disk, then in principle the disk can adjust to an approximate steady state with infall balanced by accretion. To fix ideas, we assume that the disk beyond 1 AU is mostly heated by irradiation from the central protostar of mass M_* , so that the temperature $T \propto r^{-1/2}$. For a fully viscous disk, we adopt the usual parametrization of the viscosity $\nu = \alpha c_s^2 / \Omega$, where c_s is the sound speed (for a molecular gas) and Ω is the (roughly Keplerian) angular velocity. Then

$$t_\nu \sim \frac{r^2 \Omega}{\alpha c_s^2} \sim 1.3 \times 10^3 \alpha_{-1}^{-1} M_1 T_{300}^{-1} R_{AU} \text{ yr} , \quad (2)$$

where $\alpha_{-1} \equiv \alpha/0.1$ is the viscosity parameter $M_1 \equiv M_*/M_\odot$, $R_{AU} \equiv r/\text{AU}$, and T_{300} is the temperature at 1 AU in units of 300K. From this relation we see that a fully viscous disk might be able to keep up with mass infall over typical protostellar lifetimes of $\sim 10^5$ yr if the radius at which matter is being added satisfies $R_{AU} \lesssim 10^2 \alpha_{-1}$. In a layered disk picture, the viscosity may need to be modified such that $\nu = \alpha c_s h$, where h should be the thickness of the active layer instead of the midplane scale height. However, this difference is significant only if the temperatures differ at the active layer and the midplane, which they do not unless there is some midplane viscosity. In any case, Eq. (2) provides an upper limit to R_{AU} . Since typical observational estimates of infall radii are ~ 10 -100 AU (Kenyon et al. 1993), protostellar infall to a constant α disk is likely to pile up unless α is relatively large.

A more serious problem is that protostellar disks are unlikely to have constant α . The best studied mechanism for angular momentum transport in disks, turbulence driven by the MRI (e.g., Balbus & Hawley 1998), requires a minimum ionization fraction to couple the magnetic fields to the mostly neutral disk. As substantial regions of protostellar disks will generally be too cold for thermal (collisional) ionization, ionization by nonthermal processes becomes important. This led Gammie (1996) to suggest a layered model in which non-thermally ionized surface layers are magnetically coupled while the disk midplane remain inert. We modify Gammie's analysis by assuming that the heating of the outer disk is not determined by local viscous dissipation but by irradiation from the central protostar, as above.

The mass accretion rate in a layered disk is

$$\dot{M} = 6\pi r^{1/2} \frac{\partial}{\partial r} \left(2\Sigma_a \nu r^{1/2} \right) , \quad (3)$$

where Σ_a is the (one-sided) surface density of the active layers. Taking $\Sigma_a = \text{constant}$, and assuming that the disk temperature $T \propto r^{-1/2}$,

$$\dot{M} = 5 \times 10^{-7} \Sigma_{100} T_{300} \alpha_{-1} R_{AU} , \quad (4)$$

where $\Sigma_{100} \equiv \Sigma_a / 100 \text{ g cm}^{-2}$.

Our nominal value of $\alpha = 0.1$ may be reasonable for well-ionized regions, but it may be an overestimate for the outer regions of T Tauri disks (see §5.3). Also, the fiducial value for Σ_a is based

upon Gammie’s (1996) assumption of cosmic ray ionization, which may be an overestimate due to exclusion of cosmic rays by scattering and advection in the magnetized protostellar wind. X-rays provide a higher ionization rate near the surface of the disk but are attenuated more rapidly than cosmic rays (Glassgold & Igea 1999), yielding similar or smaller Σ_a . Both calculations assume that absorption of ions and electrons by grains is unimportant, which is only true if small dust is highly depleted in the active layer (e.g., Sano et al. 2000, also Ilgner & Nelson 2006a,b,c). In summary, it is likely that the estimate in equation (4) is an upper limit, and thus it appears unlikely that the MRI can transport mass at $r \sim$ a few AU at protostellar infall rates $2 \times 10^{-6} - 10^{-5} M_\odot \text{ yr}^{-1}$. MRI transport resulting from non-thermal ionization might however move material adequately in response to infall at $r \gtrsim 10 - 100$ AU.

On the other hand, if some nonmagnetic angular momentum transport mechanism can get matter in to $r \lesssim 1$ AU, *thermal* ionization can occur and activate the MRI. A *minimum* disk temperature is given by the effective temperature generated solely by local energy dissipation

$$T > T_{eff} \sim 1600(M_1 \dot{M}_{-5})^{1/4} (R/0.2\text{AU})^{-3/4} \text{ K}, \quad (5)$$

where $\dot{M}_{-5} \equiv \dot{M}/10^{-5} M_\odot \text{ yr}^{-1}$. Radiative trapping in an optically thick disk will make internal temperatures even higher. If $T \gtrsim 1400$ K most of the silicate particles will evaporate, thus eliminating a major sink for current-carrying electrons. Therefore, high accretion rates can potentially activate the MRI on distance scales of order 1 AU or less.

If magnetic angular momentum transport is weak then mass will accumulate in the disk until the disk becomes gravitationally unstable, at which point gravitational torques can transfer mass inward. GI alone may result cause accretion outbursts (Vorobyov & Basu 2006, 2008), although the details of disk cooling are crucial in determining if such bursts actually occur due to pure GI. Moreover the GI may be unable to drive accretion in the inner disk. GI sets in when the Toomre parameter

$$Q = \frac{c_s \kappa}{\pi G \Sigma} \simeq \frac{c_s \Omega}{\pi G \Sigma} \sim 1, \quad (6)$$

where we have set the epicyclic frequency $\kappa \simeq \Omega$, appropriate for a near-Keplerian disk. At small radius Ω and c_s will be large and therefore Σ must also be large if we are to have GI. Since rapid accretion causes significant internal heating (compared to heating by protostellar irradiation), large surface densities imply significant radiative trapping, raising internal disk temperatures above the effective temperature estimate above. Thus, when considering rapid mass transfer by GI, either in a quasi-steady state or in bursts, it is necessary to consider thermal MRI activation in the inner disk.

The above considerations suggest that the only way low-mass protostellar disks can accrete steadily during infall is if a smooth transition can be made from the GI operating on scales of $\sim 1 - 10$ AU to the thermally-activated MRI at smaller radii. To test this idea, we have constructed a series of steady-state disk models with realistic opacities. We compute both MRI and GI steady models and then investigate whether a smooth, steady, or quasi-steady transition is likely. Our

results indicate that making the optimistic assumptions of steady GI and MRI accretion results in a contradiction for infall rates thought to be typical of low-mass protostars.

3. Methods

We compute steady disk models employing cylindrical coordinates (r, z) , treating radiative energy transport only in the vertical (z) direction. Energy conservation requires that

$$\sigma T_{eff}^4 = \frac{3GM_*\dot{M}}{8\pi\sigma r^3} \left(1 - \left(\frac{r_{in}}{r} \right)^{1/2} \right), \quad (7)$$

where M_* is the central star’s mass and we have assumed that the disk is not so massive as to make its rotation significantly non-Keplerian. Balance between heating by dissipation of turbulence and radiative cooling requires that

$$\frac{9}{4}\nu\rho_z\Omega^2 = \frac{d}{dz} \left(\frac{4\sigma}{3} \frac{dT^4}{d\tau} \right), \quad (8)$$

where

$$\nu = \alpha c_s^2 / \Omega \quad (9)$$

and

$$d\tau = \rho\kappa dz, \quad (10)$$

and κ is the Rosseland mean opacity. We have updated the fitting formulae provided by Bell & Lin (1994) for the Rosseland mean opacity to include more recent molecular opacities and an improved treatment of the pressure-dependence of dust sublimation (Zhu et al. 2007). The new fit and a comparison with the Bell & Lin (1994) opacity treatment is given in the Appendix.

Convection has not been included in our treatment. Lin & Papaloizou (1980) show that for a power law opacity ($\kappa = \kappa_0 T^\beta$), convection will occur when $\beta \gtrsim 1$. Our opacity calculations show that $\beta \gtrsim 1$ only occurs for $T \gtrsim 2000K$. As our steady-state analysis depends upon disk properties for $T \lesssim 1400$ K, the neglect of convection will not affect our results (see also Cassen 1993).

We ignore irradiation of the disk by the central star, as we are assuming high accretion rates and a low central protostellar luminosity. The diffusion approximation (equation 8) is adequate since the disk is optically thick at the high mass accretion rates ($\dot{M} > 10^{-7} M_\odot / yr$) we are interested in.

We also require hydrostatic equilibrium perpendicular to the disk plane,

$$\frac{dP_z}{dz} = \frac{GM_*\rho z}{r^3}, \quad (11)$$

and use the ideal gas equation of state

$$P = \frac{k}{\mu} \rho T. \quad (12)$$

Given a viscosity prescription, equations (6) - (12) can be solved iteratively for the vertical structure of the disk at each radius, resulting in self-consistent values of the surface density Σ , and the temperature at the disk midplane T_c .

In detail, we use a shooting method based on a Runge-Kutta integrator rather than a relaxation method (e.g., D’Alessio et al. 1998) to solve the two-point boundary value problem. Given α and \dot{M} at r , we fix $z = z_i$ and set $T = T_{eff}$ and $\tau = 2/3$ (this is adequate in the absence of significant protostellar irradiation), then integrate toward the midplane. We stop when the total radiative flux $= \sigma T_{eff}^4$ at $z = z_f$. In general $z_f \neq 0$; we alter the initial conditions and iterate until $z_f = 0$.

For an MRI active disk we fix $\alpha = \alpha_M$, assuming the disk is active through the entire column. We then check to see if thermal ionization is sufficient or if the surface density is low enough that non-thermal ionization is plausible. The exact temperatures above which MRI activity can be sustained are somewhat uncertain; here we assume the transition occurs for a central temperature of 1400 K, when the dust grains that can absorb ions and electrons and thus inactivate the MRI (e.g., Sano et al. 2000) are evaporated. We set $\alpha_M = 10^{-2}$ to 10^{-1} to span a reasonable range given current estimates (see §5.3).

For simplicity we neglect the possible presence of an actively accreting, non-thermally-ionized layer. This omission will not affect our results at high accretion rates, for which the layered contribution is unimportant (equation 4); our approximation then breaks down for $\dot{M} \leq 10^{-6} M_\odot \text{ yr}^{-1}$ for large values of Σ_a and α_M .

For the steady GI disk models α is not fixed. Instead we start with a large value of $\alpha = \alpha_Q$ and then vary α_Q until $Q = 2$. The adoption of the local treatment of GI energy dissipation requires some comment. Since gravity is a long-range force a local viscous description is not generally applicable (Balbus & Papaloizou 1999). However, as Gammie (2001) and Gammie & Johnson (2003) argue, a local treatment is adequate if $\lambda_c \equiv 2c_s^2/(G\Sigma) = 2\pi H Q \lesssim r$; here λ_c is the characteristic wavelength of the GI. More broadly, our main result involves order-of-magnitude arguments; that is, as long as inner disks must be quite massive to sustain GI transport, and as long as there is *some* local dissipation of energy as this transport and accretion occurs, steady accretion will not occur for a significant range of infall rates. To change our conclusions dramatically, one would need to show that the GI causes rapid accretion through the inner disk without substantial local heating. We return to this issue in §5.1.

4. Results

Figures 1a-d show steady disk results for a central star mass of $1M_\odot$ and accretion rates of 10^{-4} , 10^{-5} , 10^{-6} , and $10^{-7} M_\odot \text{ yr}^{-1}$. Proceeding counterclockwise from upper left, the panels show the central disk temperature, α_Q , the one-sided surface density $\Sigma \equiv \int_0^\infty dz \rho$, and the viscous timescale r^2/ν as a function of radius. The solid curves show results for pure-GI models, while the dotted and dashed curves show results for $\alpha_M = 0.1$ and 0.01 , respectively.

The upper left panels show that the central temperatures rise more dramatically toward small radius in the GI models than in the MRI models. The GI models have higher temperatures because their higher surface densities lead to stronger radiative trapping. The GI solutions in these high-temperature regimes are unrealistic because they assume the MRI is absent, when it seems likely the MRI will in fact be active. These high temperature states do, however, suggest the possibility of thermal instability in the inner disk at high accretion rates, especially as the solutions near ~ 3000 K represent unstable equilibria (e.g., Bell & Lin 1994; §5). We consider the MRI models to be inconsistent at $T \lesssim 1400$ K (collisional ionization would be absent) and when $\Sigma > \Sigma_a < 100 \text{ g cm}^{-2}$.

Can a smooth or steady transition between MRI and GI transport occur? The transition region would be the “plateau” in the temperature structure which occurs near $T \sim 1400$ K (see Figure 1). This plateau is a consequence of the thermostatic effects of dust opacity, which vanishes rapidly at slightly higher temperatures. A small increase in temperature past this critical temperature causes a large decrease in the disk opacity and thus the optical depth; this in turn reduces the radiative trapping and decreases the central temperature. Thus disk models tend to hover around the dust destruction temperature over roughly an order of magnitude in radius, with the plateau occurring farther out in the disk for larger accretion rates. Since the plateau is connected with the evaporation of dust, it corresponds to a region where we might expect MRI activity.³

First consider the case $\dot{M} = 10^{-4} M_{\odot} \text{ yr}^{-1}$ (upper left corner of Figure 1). The plateau region is very similar in extent for all models. More importantly, $\alpha_Q \sim 10^{-2}$ in this region, and so the surface densities of the GI and $\alpha_M = 10^{-2}$ models are nearly the same. This suggests that a steady disk solution is plausible with a transition from GI to MRI at a few AU for these parameters. Depending on the precise thermal activation temperature for the MRI, a smooth transition at around 10 AU might also occur for $\alpha_M = 0.1$.

Next consider the case $\dot{M} = 10^{-5} M_{\odot} \text{ yr}^{-1}$ (upper right corner of Figure 1). Here $\alpha_Q \sim 10^{-3}$ in the plateau region, with resulting surface densities much higher than for either of the MRI cases. This discrepancy in α and Σ between the two solutions makes a steady disk unlikely. A small increase in surface density in a GI model near the transition region, resulting in increased heating and thus thermal activation of the MRI, would suddenly raise the effective transport rates by one or two orders of magnitude, depending upon α_M . The result would be an accretion outburst. This is qualitatively the same situation as proposed for outbursts in dwarf novae, where thermal instability is coupled to an increase in α from the initial low state to the high state (similar to what Bell & Lin 1994 adopted to obtain FU Ori outbursts). Our inference of non-steady accretion also agrees with the time-dependent one-dimensional models of Armitage et al. (2001) and of Gammie (1999)

³There will be hysteresis because the dust size spectrum in a parcel of gas will depend on the parcel’s thermal history. Heating the parcel destroys the dust and the accumulated effects of grain growth. Cooling it again would presumably condense dust with small mean size (and therefore a strong damping effects on MHD turbulence). The opacity would then vary strongly with time as the grains grow again. These effects are not considered here.

and Book & Hartmann (2005), as discussed further in §5.

A similar situation holds at $10^{-6}M_{\odot}\text{yr}^{-1}$, although the evolutionary (viscous) timescales of the GI model are of order 10^5 yr, comparable to protostellar infall timescales. At this infall rate, the disk would only amass $\sim 0.1M_{\odot} = 0.1M_{*}$, and so the disk might not need to transfer this mass into the star to avoid GI. At $10^{-7}M_{\odot}\text{yr}^{-1}$, evolutionary timescales become much longer than protostellar lifetimes, and become comparable to T Tauri lifetimes; disk material can pile up without generating GI transport and consequent thermal activation of the MRI. In addition, an $\alpha_M = 0.1$ value could result in a steady disk with surface densities low enough to be activated entirely by cosmic ray or X-ray ionization. This does not mean, however, that T Tauri disks do not have layered accretion, as the surface density distribution depends upon the history of mass transport.

The results of our calculations are summarized in the $\dot{M} - r$ plane in Figure 2. The solid curves farthest to the lower right, labeled R_Q , are the radii at which the pure GI-driven disk would have a central temperature of 1400 K (at which temperature the dust starts to sublimate), and thus activate the MRI. Moving up and left, the solid curve labeled R_M denotes the radii at which a pure MRI disk of the given α_M would have a central temperature of 1400 K. When these two curves are close together, or cross, α_Q and α_M are similar, making possible a smooth transition between GI and MRI and thus steady accretion. In the (shaded) regions between these two curves the viscosity parameters diverge, making non-steady accretion likely.

The radial regions at which we predict material will pile up, trigger the MRI, and result in rapid accretion lie in the shaded regions. The dotted curve shows R_Q and R_M where the disk has a central temperature of 1800 K (at which temperature all dust has sublimated). R_Q and R_M at 1800 K are smaller than they are at 1400 K because of the plateau region discussed above. Thus if the MRI trigger temperature is higher the outbursts are expected to be shorter because the outburst drains the smaller inner disk ($r < R_Q$) on the viscous timescale.

Figure 2 indicates that non-steady accretion, with potential outbursts, is predicted to occur for infall rates $\lesssim 10^{-5}M_{\odot}\text{yr}^{-1}$ for $\alpha_M = 0.01$ and $\lesssim 10^{-4}M_{\odot}\text{yr}^{-1}$ for $\alpha_M = 0.1$. As described above, for $\dot{M} < 10^{-6}M_{\odot}\text{yr}^{-1}$ outbursts are unlikely, simply because the transport timescales are too long. Outbursts are expected to be triggered at $r \sim 1 - 10$ AU for protostellar infall rates $\sim 10^{-5} - 10^{-6}M_{\odot}\text{yr}^{-1}$. These predictions are relatively insensitive to the precise temperature of MRI activation; the dotted curves in Figure 2 show the results for a critical MRI temperature of 1400 K, which simply shift the regions of instability to slightly smaller radii without changing the qualitative results.

The other shaded band in Figure 2 denotes the region where thermal instability might occur. The two limits correspond to the two limiting values of the “S curve” (e.g., Faulkner, Lin, & Papaloizou 1983) at which transitions up to the high (rapid accretion) state and the low (slow accretion) state occur.

Figures 3-6 show results for central star masses of 0.3 and $0.05M_{\odot}$, respectively. The predictions

are qualitatively similar to the case of the $1M_{\odot}$ protostar, with the exception that thermal instability is less likely for the brown dwarf. This also implies generally unstable protostellar accretion for more massive protostars during the time that they are increasing substantially in mass.

Much of the overall behavior of our results derive from the general property that disk temperatures rise strongly toward smaller radii. For optically-thick viscous disks, the central temperatures are proportional to

$$T_c \sim T_{eff} \tau^{1/4} \propto \dot{M}^{1/4} r^{-3/4} (\kappa_R \Sigma)^{1/4}, \quad (13)$$

where τ is the vertical optical depth. Thus, even changes in surface density for differing values of α result in modest changes in radii where a specific temperature is achieved. Changing the mass accretion rate has a bigger effect, because $\Sigma \propto \dot{M}$.

5. Discussion

Our prediction of unsteady accretion during protostellar disk evolution is the result of the inefficiency of angular momentum transport of the two mechanisms considered here: the MRI, because of low ionization in the disk; and the GI, because it tends to be inefficient at small radii, where Ω and c_s will be large, forcing Σ to be large. To provide a feeling of just how large the surface density must be for $Q = 2$ in the inner disk, at accretion rates of 10^{-4} and $10^{-5} M_{\odot} \text{ yr}^{-1}$ for the $1M_{\odot}$ star the disk mass interior to 1 AU would have to be $\sim 0.6M_{\odot}$ and $\sim 0.5M_{\odot}$, respectively (Fig. 7), which are implausibly large. At some point the disk must accrete most of its mass into the star, forcing the inner disk temperatures to be very large and thermally activating the MRI, resulting in outburst of accretion. Here we consider whether the assumptions leading to this picture are reasonable, then discuss applications to outbursting systems.

5.1. Outbursts?

Our inference of cycles of outbursts of accretion - piling up of mass by GI transport, followed by thermal triggering of the MRI - was found in the models of Armitage et al. (2001), as well as in the calculations of Gammie (1999) and Book & Hartmann (2005). We have also found outbursting behavior in time-dependent two-dimensional disk models, to be reported in a subsequent paper (Zhu, Hartmann, & Gammie 2009). Here we compare our results with those of Armitage et al. .

Figure 8 shows the results of our stability calculations for parameters and opacities adopted by Armitage et al. : a central star mass of $1M_{\odot}$, $\alpha_M = 0.01$, and an assumed triggering temperature for the MRI of 800 K. Armitage et al. found steady accretion at an infall rate of $\dot{M} = 3 \times 10^{-6} M_{\odot} \text{ yr}^{-1}$ but outbursting behavior at $1.5 \times 10^{-6} M_{\odot} \text{ yr}^{-1}$. This is reasonably consistent with our calculations; R_M and R_Q are close together at $\dot{M} = 3 \times 10^{-6} M_{\odot} \text{ yr}^{-1}$ and cross near $\dot{M} = 1 \times 10^{-5} M_{\odot} \text{ yr}^{-1}$, suggesting stable accretion somewhere in this range. Armitage et al. find that the MRI is triggered

at about 2 AU, whereas our analysis (for $\dot{M} \sim 10^{-6} M_{\odot} \text{ yr}^{-1}$) would suggest a triggering radius of about 3 AU. Our ability to reproduce the results of Armitage et al. is adequate, considering that steady models do not precisely reproduce the behavior of time-dependent models, and that the form of α_Q used by Armitage et al. is somewhat different from ours, though it still retains the feature of non-negligible GI only for small Q .

Our finding of non-steady accretion is the result of assuming no other significant level of angular momentum transport that is not due to GI or thermal MRI. Terquem (2008) has shown that steady accretion is possible for a layered disk accreting at $\dot{M} = 10^{-8} M_{\odot} / \text{yr}$ if there is a non-zero (non-gravitational) viscosity in disk regions below the surface active layers. Simulations have indicated that active layers can have an effect on non-magnetically active regions below, producing a Reynolds stress promoting accretion in the lower regions (Fleming & Stone 2003; Turner & Sano 2008; Ilgner & Nelson 2008). We argue that this effect is unlikely to be important for the much higher accretion rates considered here, simply because the amount of mass transfer that needs to occur is much higher than what is sustainable by a non-thermally ionized surface layer. It seems implausible that a small amount of surface energy and turbulence generation can activate a very large amount of turbulence and energy dissipation in a much more massive region.

5.2. Local vs. non-local GI transport

We have adopted a local formalism for GI whereas it has non-local properties. Furthermore, we have adopted azimuthal symmetry in calculating the dissipation of energy whereas energy will be deposited in nonaxisymmetric spiral shocks. Neither of these assumptions is strictly correct.

Boley et al. (2006) performed a careful analysis of the torques in a three-dimensional model of a self-gravitating disk, including radiative transfer. They found that the mass transfer was dominated by global modes, but could be consistent with a locally-defined $\alpha(r, t)$. This result did not hold near the inner and outer edge of their disk, although this is not surprising as these regions were characterized by $Q > 2$ and thus one would not expect the GI to be operating. Boley et al. were unable to address whether energy dissipation was localized. Nevertheless it is difficult to imagine that gravitational instability could avoid some heating in regions with $Q \sim 1$, and only relatively small amounts of heating are required to activate the MRI at small radii.

The details of the disk temperature structure near 1 AU must be found by three dimensional simulations of the GI with realistic cooling. The analysis presented here suggests that pure GI in the absence of MRI tends to lead to very long transport times in the inner disk, as required by our low values of α_Q . This presents two potential technical problems for a numerical investigation: first, numerical viscosity must be smaller than α_Q to follow the evolution; and second, the disk must be followed over long, evolutionary timescales. It will be challenging to follow the GI near 1 AU numerically.

5.3. What is α_M ?

The magnetic transport rate α_M is constrained by both observations and theory. A recent review of the observational evidence by King, Pringle, & Livio (2007) argues that α_M must be large, of the order 0.1-0.4, based in part on observations of dwarf novae and X-ray binaries where there is no question of gravitational instability. Our own analysis required $\alpha \sim 0.1$ in FU Ori (Zhu et al. 2007).

On the theoretical side the situation is murky. Early calculations (Hawley et al. 1996) suggested that for “shearing box” models with zero mean azimuthal and vertical field $\alpha_M \simeq 0.01$. Recent work (Fromang & Papaloizou 2007), however, shows that α_M does not converge in the sense that $\alpha_M \rightarrow 0$ as the numerical resolution increases.

But are the zero mean field models relevant to astrophysical disks? Global disk simulations (Hirose et al. 2004; McKinney & Narayan 2007; Beckwith et al. 2008), local disk simulations in which the mean field is allowed to evolve because of the boundary conditions (Brandenburg et al. 1995), and observations of the galactic disk (Vallee 2004) all exhibit a “mean” azimuthal field when an average is taken over areas of $\gtrsim H^2$ in the plane of the disk. This suggests that the zero mean field local models are a singular case, and that mean azimuthal field models are most relevant to real disks (strong vertical fields would appear to be easily removed from disks according to the plausible phenomenological argument originally advanced by van Ballegoijen (1989)).

So what do numerical simulations tell us about disks with mean azimuthal field? Recent work shows that in this case the outcome depends on the magnetic Prandtl number $Pr_M \equiv \nu/\eta$ (Fromang et al. 2007; Lesur & Longaretti 2007) ($\nu \equiv$ viscosity and $\eta \equiv$ resistivity) and that α_M is a monotonically increasing function of Pr_M . This intriguing result, and the fact that YSO disks have $Pr_M \ll 1$ throughout (although more dimensionless parameters are required to characterize YSO disks, where the Hall effect and ambipolar diffusion can also be important), might suggest that α_M should be small. But the numerical evidence also shows that α_M depends on ν in the sense that the dependence on Pr_M weakens as ν decreases. In sum, the outcome is not known as ν drops toward astrophysically plausible values. Mean azimuthal field models with effective $Pr_M \sim 1$ Guan et al. (2008) are also not fully converged; they show that α_M *increases*, albeit slightly, as the resolution is increased. For a mean field with plasma $\beta = 400$ Guan et al. (2008) find $\alpha_M = 0.03$ at their highest resolution. In disks with an initial strong azimuthal magnetic field in equipartition with thermal pressure, Johansen & Levin (2008) find $\alpha = 0.1$ resulting from a combination of the Parker instability and an MRI-driven dynamo.

Very small α_M would pose a problem for T Tauri accretion. In the layered disk model, Gammie estimated the accretion rate to be

$$\dot{M} \sim 2 \times 10^{-8} \left(\frac{\alpha_M}{0.01} \right)^2 \left(\frac{\Sigma_a}{100 \text{ g cm}^{-2}} \right)^3 \text{ M}_\odot \text{ yr}^{-1}, \quad (14)$$

where Σ_a is the surface density of the layer which is non-thermally ionized. Thus with $\alpha_M \lesssim 10^{-3}$

it would be difficult to explain typical T Tauri accretion rates.

On the other hand $\alpha_M \sim 0.1$ could cause the outer disks of T Tauri stars to expand to radii of 1000 AU or more in 1 Myr (Hartmann et al. 1998). There is no particular reason why the $\alpha_M \sim 0.1$ that we estimated for the thermally-ionized inner disk region in FU Ori should be the same as the effective α in the outer disks of T Tauri stars, which cannot be thermally ionized.

5.4. Protostellar accretion

Our models predict that most low-mass protostars will be accreting more slowly than matter is falling onto their disks. This is consistent with observational results, as outlined in the Introduction. The results of Armitage et al. (2001) suggested that steady accretion might be possible at $\sim 3 \times 10^{-6} M_\odot \text{ yr}^{-1}$ and above (for $1 M_\odot$). We find a different result because we adopt a significantly higher temperature for thermal MRI activation, closer to that required for dust evaporation. This means that our MRI triggering occurs at smaller radii, where the GI is less effective. It does seem likely that higher activation temperatures than the 800 K adopted by Armitage et al. are more plausible. Even if thermal ionization in the absence of dust is sufficient at around 1000 K in statistical equilibrium, ionization rates are so low that equilibrium is unlikely (e.g. Desch 1998). We also note that Armitage et al. were unable to obtain the high accretion rates and short outburst durations characteristic of FU Ori objects, but Book & Hartmann (2005) were able to reproduce the FU Ori characteristics better with a higher MRI activation temperature.

At infall rates $\gtrsim 10^{-4} M_\odot \text{ yr}^{-1}$, our models predict (quasi-) steady accretion (also Armitage et al. 2001); but such high rates are not expected to last long, perhaps only during an initial rapid phase of infall (Foster & Chevalier 1993; Hartmann et al. 1994; Henriksen, Andre, & Bontemps 1997). Testing this prediction may be difficult as relatively few objects will be caught in this phase and they will likely be heavily embedded.

At lower infall rates, GI-driven accretion timescales are longer than evolutionary times and/or layered MRI turbulence may produce sufficient mass transport. Thus, we would not expect outbursts for Class II (T Tauri) stars.

5.5. FU Ori outbursts

In our radiative transfer modeling of the outbursting disk system FU Ori (Zhu et al. 2007), we found that to fit the *Spitzer Space Telescope* IRS spectrum the rapidly-accreting, hot inner disk must extend out to ~ 1 AU, inconsistent with a pure thermal instability model. In contrast, the results of this paper suggest thermal MRI triggering can occur at a few AU, in much better agreement with observation.

Our recent analysis of the silicate emission features of FU Ori (Zhu et al. 2008) also suggests

that the disk becomes dominated by irradiation rather than internal heating at distances of $\gtrsim 1$ AU, but this is consistent with the results of this paper, as irradiation from the central disk can dominate local viscous dissipation if the disk is sufficiently flared.

We also found that the decay timescales of FU Ori suggest $\alpha_M \sim 10^{-1}$; large values of α_M are more likely to lead to outbursting behavior. High inner disk accretion rates also make thermal instability more likely very close to the central star; the presence or absence of this instability may account for the difference in rise times seen in some FU Ori objects (Hartmann & Kenyon 1996).

6. Conclusions

Our study predicts that the disk accretion of low-mass protostars will generally be unsteady for typical infall rates. During the protostellar phase, GI is likely to dominate at radii beyond 1 AU but not at smaller radii; in contrast, rapid accretion should drive thermal activation of the MRI in the inner disk. Because of the differing transport rates comparable to typical infall values results in high inner disk temperatures sufficient to trigger the MRI. This is a general conclusion, though if the external disk accretion is driven by GI, the radius at which the MRI can be triggered thermally is much larger, because of the high surface density needed to produce a low value of Q . Furthermore, GI-driving in the inner disk results in a low value of α_Q , much lower than the expected α_M , for a wide range of \dot{M} . The feature of mass accumulation at low external α followed by a change to a high inner viscosity is similar to thermal instability models (and also Armitage et al. 2001). Thermal instabilities may also occur in the inner disk at very high accretion rates, enhancing the potential for non-steady protostellar accretion.

A. Appendix: Rosseland mean opacity

The Bell & Lin (1994) Rosseland mean opacity fit has been widely used to study high temperature accretion disks (CV objects, FU Ori, et al.) for more than a decade, with opacities generated almost two decades ago. Our understanding of opacity sources (especially dust and molecular line spectra) has improved both observationally and theoretically since then (Alexander & Ferguson 1994; Ferguson et al. 2005; D’Alessio et al. 1998, 2001; Zhu et al. 2007).

We have generated Rosseland mean opacity assuming LTE for a wide range of temperature and pressure during our study of FU Orionis objects (Zhu et al. 2007, 2008). The molecular, atomic, and ionized gas opacities have been calculated using the Opacity Distribution Function (ODF) method (Castelli & Kurucz 2004; Sbordone et al. 2004; Castelli 2005; Zhu et al. 2007) which is a statistical approach to handling line blanketing when millions of lines are present in a small wavelength range (Kurucz et al. 1974). The dust opacity was derived by the prescription in D’Alessio et al. (2001) (Zhu et al. 2008). Our opacity has been used not only to study FU Orionis objects but also to fit the gas opacity for Herbig Ae star disks constrained by interferometric observations (Tannirkulam et al.

2008). The opacities are shown in Figure 9). Compared with Alexander & Ferguson (1994) or Zhu et al. (2007,2008), the Bell & Lin opacity lacks water vapor and TiO opacity around 2000 K and has a lower dust sublimation temperature.

We have made a piecewise power-law fit to the Zhu et al. (2007, 2008) opacity (analogous to the Bell & Lin fit) to enhance computational efficiency (Table 1; see also Figure 9). This speedup has been useful in performing the calculations of this paper, and is essential for our forthcoming two-dimensional hydrodynamic simulations of FU Ori outbursts (Zhu, Hartmann, & Gammie 2009).

We acknowledge useful conversations with Ken Rice and Dick Durisen. This work was supported in part by NASA grant NNX08A139G, by the University of Michigan, and by a Sony Faculty Fellowship, a Richard and Margaret Romano Professorial Scholarship, and a University Scholar appointment to CG.

REFERENCES

- Alexander, D. R., & Ferguson, J. W. 1994, *ApJ*, 437, 879
- Andre, P., Ward-Thompson, D., & Barsony, M. 2000, *Protostars and Planets IV*, 59
- Armitage, P. J., Livio, M., & Pringle, J. E. 2001, *MNRAS*, 324, 705
- Balbus, S. A., & Papaloizou, J. C. B. 1999, *ApJ*, 521, 650
- Bally, J., Reipurth, B., & Davis, C. J. 2007, *Protostars and Planets V*, 215
- Bate, M. R., Bonnell, I. A., & Bromm, V. 2003, *MNRAS*, 339, 577
- Beckwith, K., Hawley, J. F., & Krolik, J. H. 2008, *ApJ*, 678, 1180
- Bell, K. R., & Lin, D. N. C. 1994, *ApJ*, 427, 987
- Boley, A. C., Mejía, A. C., Durisen, R. H., Cai, K., Pickett, M. K., & D’Alessio, P. 2006, *ApJ*, 651, 517
- Book, L. G., & Hartmann, L. 2005, *BAAS*, 37, 1287
- Brandenburg, A., Nordlund, A., Stein, R., & Torkelsson, U. 1995, *ApJ*, 446, 741
- Cai, K., Durisen, R. H., Boley, A. C., Pickett, M. K., & Mejía, A. C. 2008, *ApJ*, 673, 1138
- Cassen, P. 1993, *Lunar and Planetary Institute Conference Abstracts*, 24, 261
- Castelli, F. 2005, *Memorie della Societa Astronomica Italiana Supplement*, 8, 34
- Castelli, F., & Kurucz, R. L. 2004, *ArXiv Astrophysics e-prints*, arXiv:astro-ph/0405087

- Clarke, C. J., & Syer, D. 1996, MNRAS, 278, L23
- D’Alessio, P., Calvet, N., & Hartmann, L. 2001, ApJ, 553, 321
- D’Alessio, P., Canto, J., Calvet, N., & Lizano, S. 1998, ApJ, 500, 411
- Desch, S. J. 1998, Ph.D. Thesis, U. Illinois.
- Faulkner, J., Lin, D. N. C., & Papaloizou, J. 1983, MNRAS, 205, 359
- Ferguson, J. W., Alexander, D. R., Allard, F., Barman, T., Bodnarik, J. G., Hauschildt, P. H., Heffner-Wong, A., & Tamanai, A. 2005, ApJ, 623, 585
- Fleming, T., & Stone, J. M. 2003, ApJ, 585, 908
- Foster, P. N., & Chevalier, R. A. 1993, ApJ, 416, 303
- Fromang, S., & Papaloizou, J. 2007 \dot{a} , 476, 1113 (FP07)
- Fromang, S., Papaloizou, J., Lesur, G., & Heinemann, T. 2007, A&A, 476
- Furlan, E., et al. 2008, ApJS, 176, 184
- Gammie, C. F. 1996, ApJ, 457, 355
- Gammie, C. F. 2001, ApJ, 553, 174
- Guan, Gammie, C. F. et al. 2008, in preparation
- Johnson, B. M., & Gammie, C. F. 2003, ApJ, 597, 131
- Gammie, C. F. 1999, ASP Conference series 160, 122
- Guan, X., Gammie, C. F., Simon, J., and Johnson, B. M. 2008, ApJ, in prep.
- Glassgold, A. E., Najita, J., & Igea, J. 1997, ApJ, 480, 344
- Hartmann, L., Boss, A., Calvet, N., & Whitney, B. 1994, ApJ, 430, L49
- Hartmann, L., Cassen, P., & Kenyon, S. J. 1997, ApJ, 475, 770
- Hartmann, L., & Kenyon, S. J. 1996, ARA&A, 34, 207
- Hawley, J. F., Gammie, C. F., & Balbus, S. A. 1995, ApJ, 440, 742
- Hawley, J. F., Gammie, C. F., & Balbus, S. A. 1996, ApJ, 464, 690
- Henriksen, R., Andre, P., & Bontemps, S. 1997, A&A, 323, 549
- Herbig, G. H. 1977, ApJ, 217, 693

- Hirose, S., Krolik, J., De Villiers, J.-P., & Hawley, J. 2005, *ApJ*, 606, 1083
- Ilgner, M., & Nelson, R. P. 2006a, *A&A*, 445, 205
- Ilgner, M., & Nelson, R. P. 2006b, *A&A*, 445, 223
- Ilgner, M., & Nelson, R. P. 2006c, *A&A*, 455, 731
- Ilgner, M., & Nelson, R. P. 2008, *A&A*, 483, 815
- Johansen, A., & Levin, Y. 2008, *A&A*, 490, 501
- Kenyon, S. J., Calvet, N., & Hartmann, L. 1993, *ApJ*, 414, 676
- Kenyon, S. J., Hartmann, L. W., Strom, K. M., & Strom, S. E. 1990, *AJ*, 99, 869
- Kenyon, S. J., Gomez, M., Marzke, R. O., & Hartmann, L. 1994, *AJ*, 108, 251
- King, A. R., Pringle, J. E., & Livio, M. 2007, *MNRAS*, 376, 1740
- Kurucz, R. L., Peytremann, E., & Avrett, E. H. 1974, Washington : Smithsonian Institution : for sale by the Supt. of Docs., U.S. Govt. Print. Off., 1974., 37
- Lesur, G., & Longaretti, P.-Y. 2007, *MNRAS*, 378, 1471
- Lin, D. N. C., Faulkner, J., & Papaloizou, J. 1985, *MNRAS*, 212, 105
- Lin, D. N. C., & Papaloizou, J. 1980, *MNRAS*, 191, 37
- Lin, D. N. C., & Papaloizou, J. 1985, *Protostars and Planets II*, 981
- Lodato, G., & Clarke, C. J. 2004, *MNRAS*, 353, 841
- McKinney, J. C., & Narayan, R. 2007, *MNRAS*, 375, 513
- Muzerolle, J., Hartmann, L., & Calvet, N. 1998, *AJ*, 116, 2965
- Myers, P. C., Adams, F. C., Chen, H., & Schaff, E. 1998, *ApJ*, 492, 703
- Tannirkulam, A., et al. 2008, *ArXiv e-prints*, 808, arXiv:0808.1728
- Sano, T., Miyama, S. M., Umebayashi, T., & Nakano, T. 2000, *ApJ*, 543, 486
- Sbordone, L., Bonifacio, P., Castelli, F., & Kurucz, R. L. 2004, *Memorie della Societa Astronomica Italiana Supplement*, 5, 93
- Shu, F. H., Adams, F. C., & Lizano, S. 1987, *ARA&A*, 25, 23
- Stahler, S. W. 1988, *ApJ*, 332, 804

- Terquem, C. E. J. M. L. J. 2008, arXiv:0808.3897
- Turner, N. J., & Sano, T. 2008, ApJ, 679, L131
- Vallee, J. P. 2004, NewA Rev., 48, 763
- van Ballegooijen, A. A. 1989, Accretion Disks and Magnetic Fields in Astrophysics, 156, 99
- Vorobyov, E. I., & Basu, S. 2005, ApJ, 633, L137
- Vorobyov, E. I., & Basu, S. 2006, ApJ, 650, 956
- Vorobyov, E. I., & Basu, S. arXiv:0802.2242v1
- bibitem[White et al.(2007)]2007prpl.conf..117W White, R. J., Greene, T. P., Doppmann, G. W., Covey, K. R., & Hillenbrand, L. A. 2007, Protostars and Planets V, 117
- White, R. J., & Hillenbrand, L. A. 2004, ApJ, 616, 998
- Zhu, Z., Hartmann, L., Calvet, N., Hernandez, J., Muzerolle, J., & Tannirkulam, A.-K. 2007, ApJ, 669, 483
- Zhu, Z., Hartmann, L., Calvet, N., Hernandez, J., Tannirkulam, A.-K., & D’Alessio, P. 2008, ArXiv e-prints, 806, arXiv:0806.3715 (ApJ, in press)

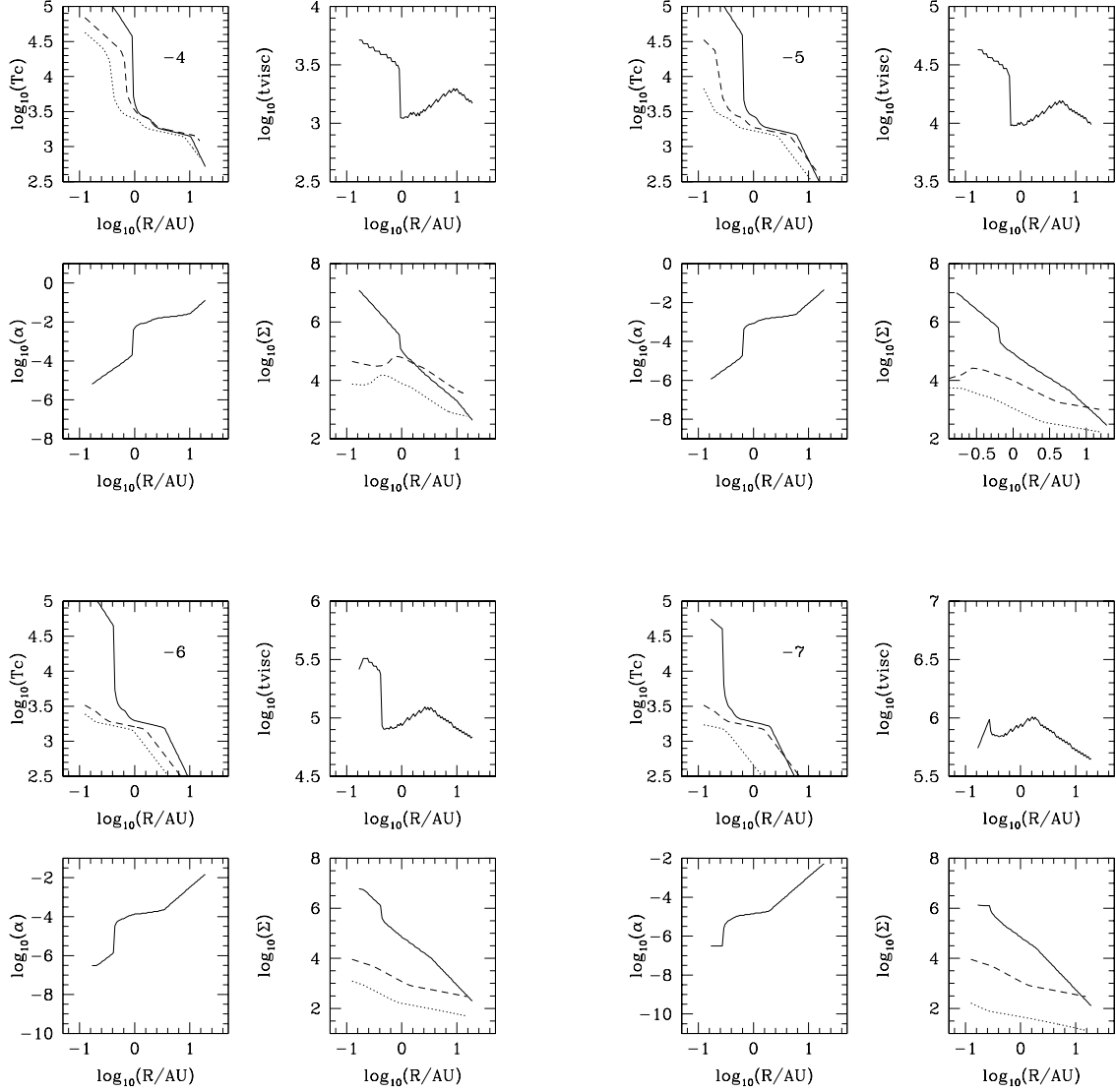


Fig. 1.— Steady-state disk calculations for four accretion rates - 10^{-4} , 10^{-5} , 10^{-6} , and $10^{-7} M_{\odot} \text{ yr}^{-1}$, assuming a central star of mass $1 M_{\odot}$. The solid curves show solutions for GI-driven accretion, as described in the text. The dashed and dotted curves yield results for steady disk models with a constant $\alpha = 10^{-2}$ and 10^{-1} , respectively (see text)

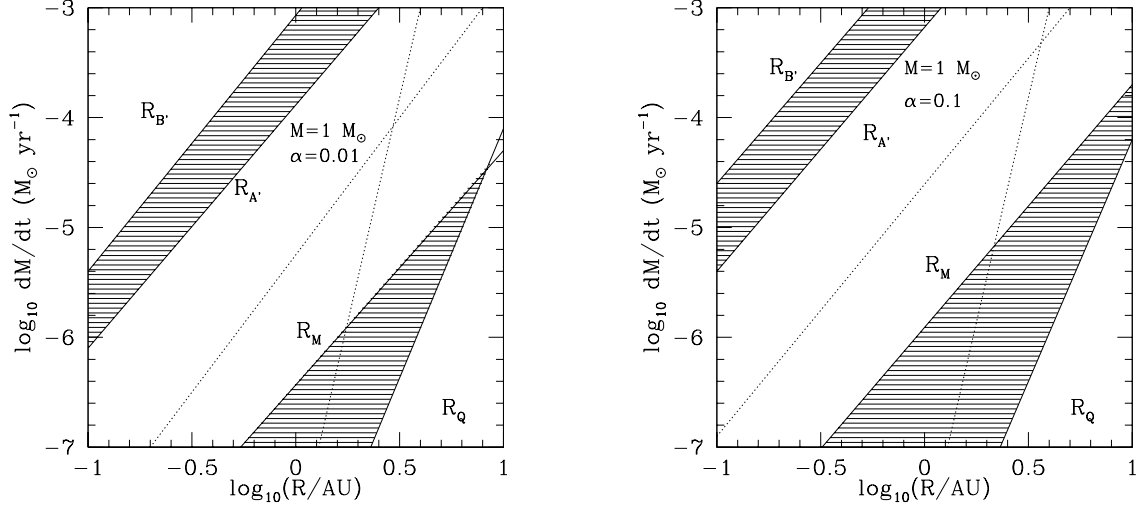


Fig. 2.— Unstable regions in the $r - \dot{M}$ plane for a 1M_\odot central star. The shaded region in the lower right shows where the central temperature of steady GI models exceeds an assumed MRI trigger temperature of 1400 K. The dotted curves show R_M and R_Q (the boundaries of the shaded region; see text for definition) for an MRI trigger temperature of 1800 K. The shaded region in the upper left shows the region subject to classical thermal instability.

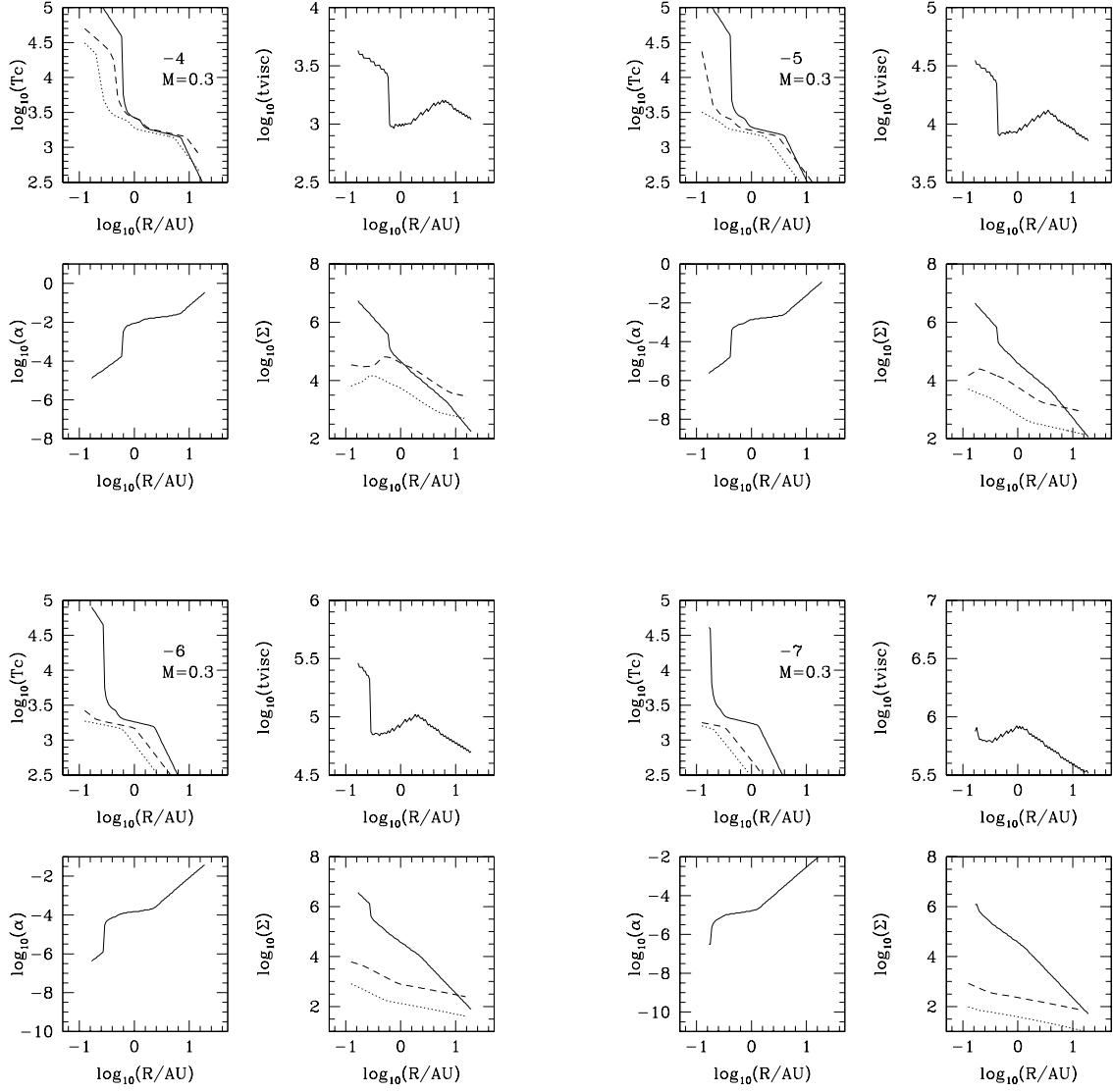


Fig. 3.— Same as in Figure 1 but for a central star mass of $0.3M_{\odot}$.

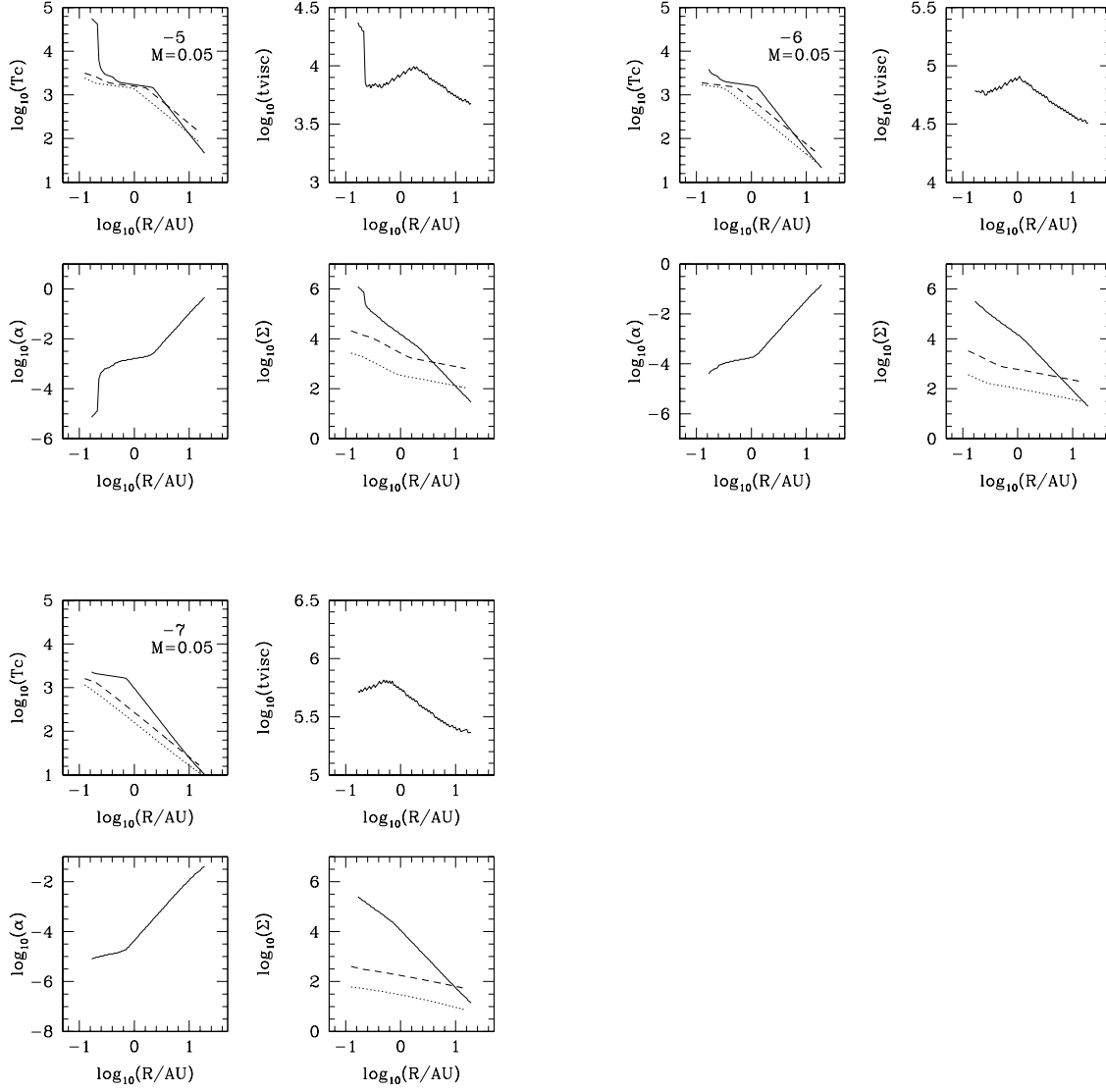


Fig. 4.— Same as in Figure 1 but for a central star mass of $0.05M_{\odot}$.

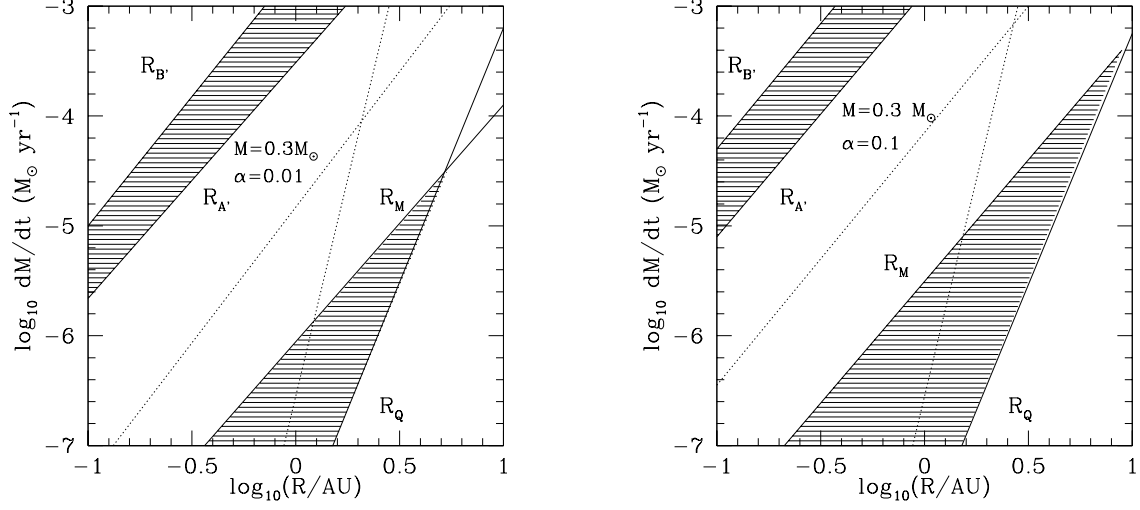


Fig. 5.— Same as figure 2 for $0.3M_{\odot}$ central star.

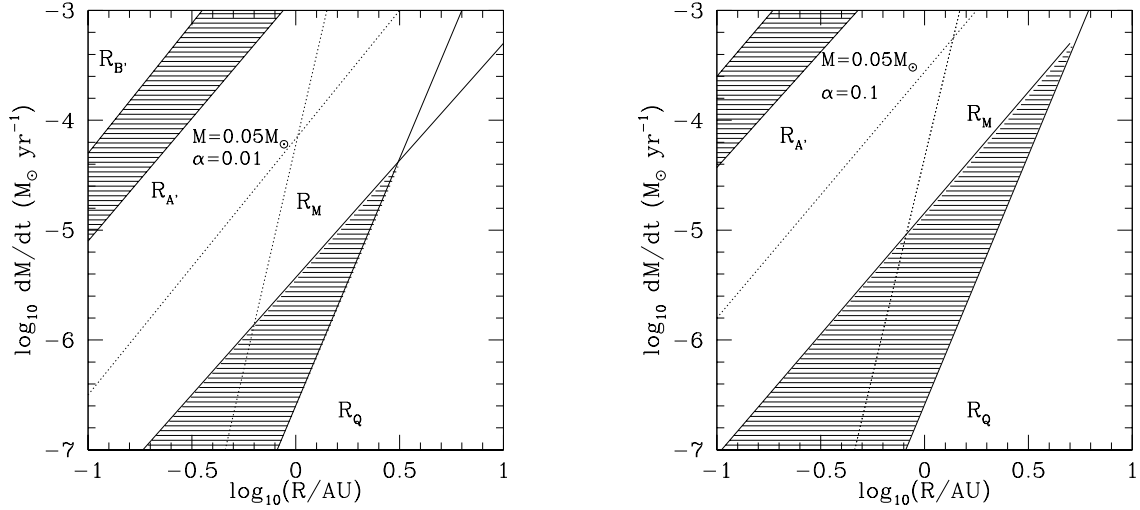


Fig. 6.— Same as Figure 2 for the $0.05M_{\odot}$ central star.

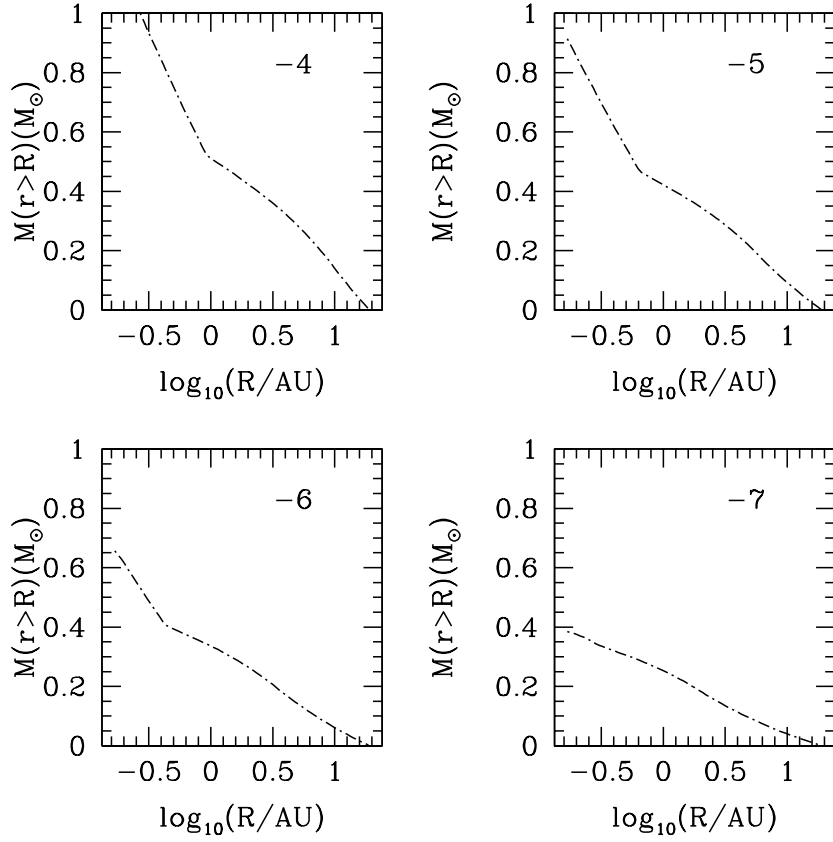


Fig. 7.— The mass of the disk integrated between radius R and the outer radius of 20 AU for steady-state $Q=2$ disks, at four accretion rates - 10^{-4} , 10^{-5} , 10^{-6} , and $10^{-7} M_\odot \text{yr}^{-1}$. The central star mass is $1 M_\odot$.

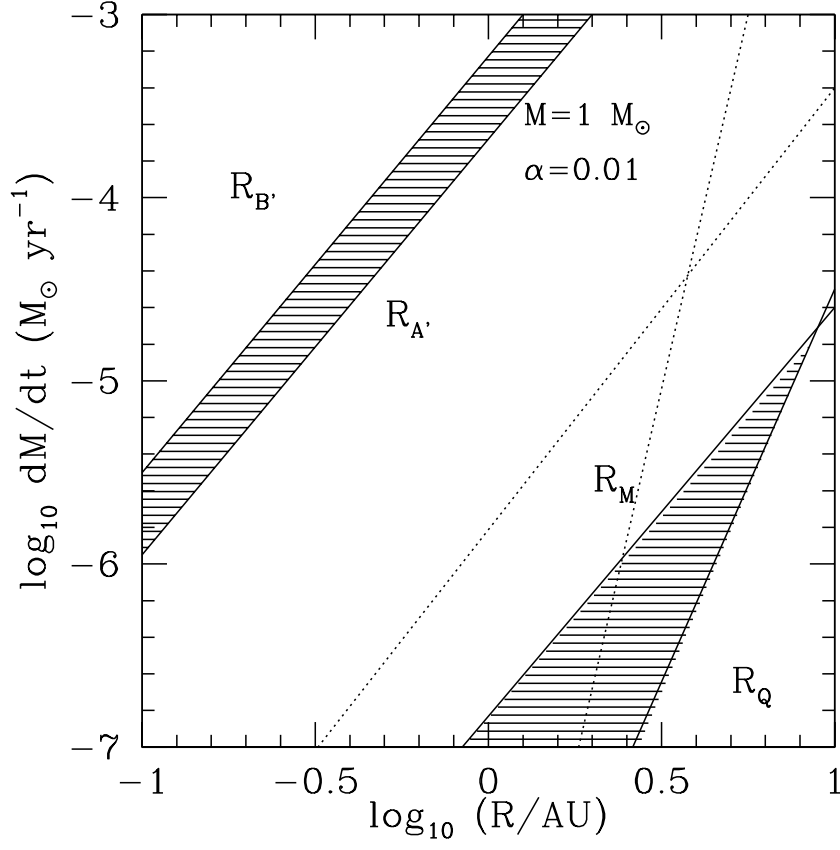


Fig. 8.— Same as Figure 2 for the parameters of Armitage et al. (2001) (see text)

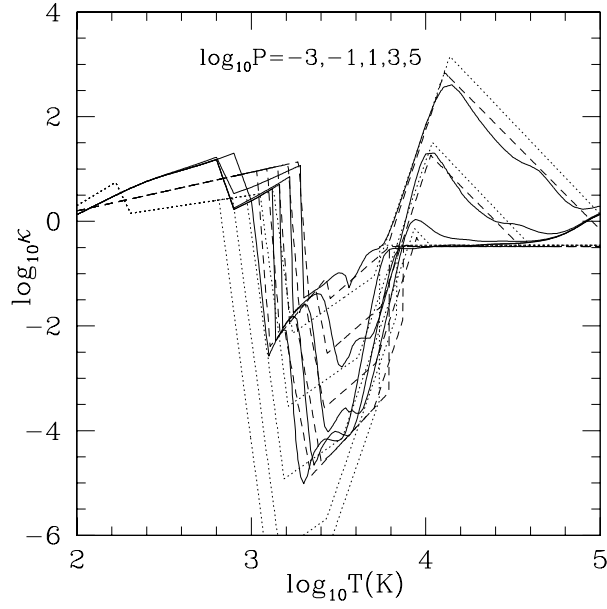


Fig. 9.— Rosseland mean opacities: the dotted lines show the Bell & Lin (1994) fit, the solid curves show the detailed opacity calculation of Zhu et al. (2007, 2008) (solid line), and the dashed lines show the simple fit to Zhu et al. opacities (Table 1).

Table 1: Fit to Zhu et al. (2007, 2008) opacity

$\log_{10} T$	$\log_{10} \kappa$	comments
$< 0.03 \log_{10} P + 3.12$	$0.738 \log_{10} T - 1.277$	grain opacity
$< 0.0281 \log_{10} P + 3.19$	$-42.98 \log_{10} T + 1.312 \log_{10} P + 135.1$	grain evaporation
$< 0.03 \log_{10} P + 3.28$	$4.063 \log_{10} T - 15.013$	water vapor
$< 0.00832 \log_{10} P + 3.41$	$-18.48 \log_{10} T + 0.676 \log_{10} P + 58.93$	
$< 0.015 \log_{10} P + 3.7$	$2.905 \log_{10} T + 0.498 \log_{10} P - 13.995$	molecular opacities
$< 0.04 \log_{10} P + 3.91$	$10.19 \log_{10} T + 0.382 \log_{10} P - 40.936$	H scattering
$< 0.28 \log_{10} P + 3.69$	$-3.36 \log_{10} T + 0.928 \log_{10} P + 12.026$	bound-free, free-free
else ^a	-0.48	electron scattering

^awith two additional condition to set the boundary: if $\log_{10} \kappa < 3.586 \log_{10} T - 16.85$ and $\log_{10} T < 4$, $\log_{10} \kappa = 3.586 \log_{10} T - 16.85$; if $\log_{10} T < 2.9$, $\log_{10} \kappa = 0.738 \log_{10} T - 1.277$